Indian J. Phys. **78A** (2), 151-157 (2004)

Nanomaterials–2003

AN INTERNATIONAL JURNA
IJP A

Nanoscale magnetic multilayers : density functional calculations

G P Das

Technical Physics & Prototype Engineering Division,
Bhabha Atomic Research Centre, Mumbai-400 085, India

E-mail gpd@magnum.barc.ernet.in

Abstract In nanostructured materials and devices, the basic principle lies in geometric confinement and proximity effects, which are size-related quantum effects. The former can be realized in two-dimensional, one-dimensional or zero dimensional confinements as can be respectively seen in epitaxial interfaces/quantum wells, quantum wires and quantum dots. While the later can be found in atomically engineered array of quantum dots on some substrate, or multilayers (superlattices) of alternate metallic (semi-conducting) A/B planes. In this paper, I shall discuss how first-principles density functional calculations can be used to probe such nanostructures. In particular, I shall focus on magnetic multilayers where confinement of electrons in a quantum well formed in the nonmagnetic layer by the spin-dependent potentials of the magnetic layers gives rise to the GMR effect which is exploited in the magnetoelectronic devices. Two of the most widely studied magnetic multilayer systems *viz.* Ni/Cu and Fe/Cr will be taken up as case studies.

Keywords Metallic multilayers, nanoscale simulations, TB-LMTO electronic structure, giant magnetoresistance

PACS Nos. 73.21.Ac, 73.22.-f, 75.47.De, 75.70.-i

1. Introduction

Nanoscale materials are broadly, rather somewhat loosely, defined as that class of materials which has one or more physical dimension smaller than 100 nanometer (*i.e.* 0.1 μ). By this yardstick, there are several examples of nanomaterials starting from integrated circuits to magnetic recording and memory devices to quantum dots and wires [1]. Structures in the nanometer dimension are fundamentally different because they fall in the domain of quantum length scale. Properties of materials depend not only on their crystal structure, chemical composition, thermodynamics phase, but also on their size and dimensionality. It is well known from dimensional considerations that electronic density of states has different energy dependencies in 3D, 2D, 1D and 0D. Therefore there are also related differences for the Fermi energy, Fermi wavevector, and so on. These dimensionality effects play important roles in various areas of science. Size-dependent evolution of properties from molecular to condensed (bulk) phase is getting increasing attention in this field of nanomaterials. For example, in metallic multilayers exhibiting novel magnetic properties, the electron exchange length governing cooperative magnetic response is ~ few lattice spacing (~ nm). Similarly, in semiconductor nanostructure, quantum dots *etc*, the spatial dimension may go to ~ a few tens of nm. Recently IBM researchers [2] have reported producing transistors out of carbon nanotubes that can outperform similar silicon transistors, thereby breaking the physical barrier of 70 nm width of gate electrode that is expected to occur in this decade. The ability to fabricate such nanostructures coupled with the advent of highly powerful atomic scale simulation technique have contributed to the proliferation of this field of nanoscience and nanotechnology. Precise control and manipulation in the atomistic level to create novel structures with unique physical and chemical properties, require a deep understanding as to how they originate. There are two distinct approaches to produce nanoscale materials [3] *viz.* (a) 'top-down' approach *i.e.* to etch or machine small features into an existing structure using techniques such as STM, AFM, electron beam lithography *etc.* and (b) 'bottom-up' approach *i.e.* build up tiny structures from even smaller molecular components *via* chemical self-assembly, molecular beam epitaxy *etc.* It is particularly this later approach that gets complimented by computer simulation and modeling where the nanostructure is generated atom by atom, molecule by molecule, plane by plane.

We are going to address here a specific class of 2D nanostructured material where the confinement is only along one direction. Epitaxial interfaces, polytypes, multilayers, superlattices and quantum well structures all fall within this broad class of nanostructures. Semiconductor superlattices for example, introduced by Esaki and Tsu [4] are man-made periodic structures consisting of thin alternate layers of two

semiconductors which may or may not have matching lattice constants. In these periodic structures, the layer thickness is typically of the order of a few nanometers (less than electron mean free path but greater than the interatomic spacing). A number of well developed sophisticated techniques such as molecular beam epitaxy, metal-organic chemical vapor deposition, laser ablation *etc*. have been deployed for growing such systems. In this paper we shall discuss the problem of metallic multilayers where the magnetic coupling between two magnetic layers separated by a non-magnetic metallic spacer layer gets manifested due to confinement of electrons in the quantum well. There is an interesting interplay between confinement and proximity effects in these systems.

2. Methodologies for nanoscale simulations

Computer simulation plays the crucial role of explaining (producing meaningful numbers) as well as predicting the experimental result, and also helps narrowing down the various experimental possibilities. It is a theoretical challenge to simulate physical properties, such as electronic, magnetic, phononic, optical, transport *etc*. of nanoscale materials [5], because of several reasons.

(a) The well-established k-space band structure techniques as applied to ordered or chemically disordered solids can not be straight-forwardly extended to spatially confined systems where the periodicity is essentially broken [6]. There are, of course, some favorable cases that are amenable *via* supercell band structure approach, as will be considered in the following section of this article.

(b) The highly accurate quantum chemical methods [7] used for molecular systems become unmanageably heavy to be applied to nanomaterials involving hundreds or thousands of atoms.

(c) Approaches based on fragmentation of a system into smaller subsystems whose wave functions, electron densities and total energies are judiciously joined together, have limited applicabilities; *e.g*. such approach has been successfully applied to some prototype biological systems [8,9].

(d) Combined classical-quantum approaches, where the appropriate quantum mechanical equations are solved in the so-called 'active region' while the 'surrounding environment' is treated classically [10], are having limited accuracy-cum-applicability as of today.

(e) The evolutionary search approach combined with first-principles calculations, which was successfully applied to narrow down the number of 'experiments' needed for the development of new superalloys [11], is yet to be attempted on functional nanomaterials.

While there is no unique prescription for simulating nanostructured systems, one should keep in kind two conflicting requirements *viz*. the size of the system (*i.e*. number of atoms) and the level of accuracy required (in say total energy or force). Computational effort increases with either of these two. There are three broad classes of methods with decreasing levels of sophistication *viz*. (a) Hartree-Fock (HF) or quantum monte carlo (QMC) or density functional (DFT) based *ab initio* methods, which can handle 10^1–10^2 atom, (b) semi-empirical tight-binding methods which can handle 10^2–10^3 atoms and (c) embedded atom or effective medium approaches which can handle $\geq 10^4$ atoms. Here, we shall focus on local density functional [12–14] based electronic structure methods which are supposed to be the most versatile and reasonably accurate. In particular, the tight-binding LMTO method [15] is an ideal tool for treating 2D nanostructure systems such as epitaxial interfaces and multilayers that can be modeled using large supercells with low symmetry [16]. For a simplified description of this approach and its usefulness in first-principle design of materials including hetero-interfaces, the reader is referred to two recent reviews [17,18].

In any multilayer structure formed by sequentially growing two or more solids, the electronic structure is perturbed locally near the interface, while it reduces to that of the individual solids a few layers away from the interface. Due to charge transfer between the two solids, an interface induced dipole is created leading to an energy line-up of the two band structures. The dipole is defined as the difference between the two asymptotic values of the average point-charge potential at both sides of the heterojunctions *i.e*. $D = V(\infty) - V(-\infty)$. In order to estimate the band offsets in semiconductor heterojunctions or Schottky barrier heights in metal/semiconductor interfaces, the calculation of this interface induced dipole is very crucial [16,19]. However, for metal-metal contacts, this problem is relatively simple because both dielectric constants are infinite so that no long-range dipole can exist in the system, and the two Fermi levels only should align in order to ensure local charge neutrality [20].

3. Metallic multilayers

Interesting electronic, magnetic, optical, elastic and superconducting properties get manifested when two or more metals form multilayer structure [21]. However, the most startling discovery was giant magnetoresistance (GMR) in Fe/Cr multilayers [22]. The phenomenon of GMR gets manifested in thin ferromagnetic (FM) layers A_m (A = Fe, Co, Ni) separated by non-magnetic (NM) or antiferromagnetic (AFM) metal interlayers B_n (B = Cu, Cr *etc*.), where m and n are the corresponding number of atomic layers. The spacer layer couples to the otherwise FM layers *via* the RKKY superexchange resulting in AFM ordering of magnetic layers, and it is the AFM coupling that gives rise to GMR [23,24]. The basic principle of GMR is schematically illustrated [25] in Figure 1. At zero field, magnetization of F layers are anti-parallel (AP) due to non-local exchange coupling.

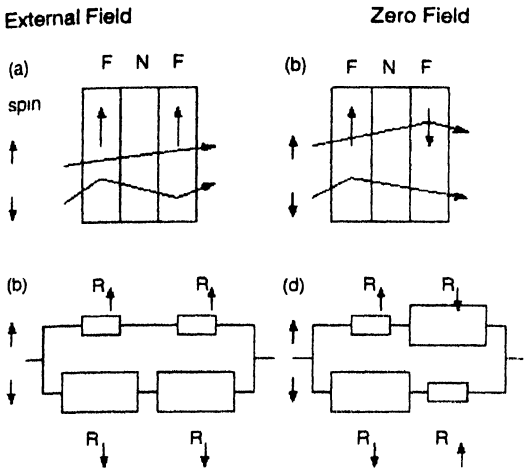

Figure 1. Origin of GMR in terms of spin-dependent electron scattering. At zero magnetic field the magnetizations in the multilayer must be aligned anti-parallel as in (b), but can be switched by a weak applied field to a parallel orientation as in (a). The equivalent resistance circuits corresponding to the situation (a) and (b) [in the top panel], are given in (c) and (d) respectively [in the bottom panel]

Application of an external field forces the magnetization of the F layers to be oriented in parallel (P). When the AP-alignment of the adjacent layers at zero field is changed to a P-alignment by an external magnetic field, there is a drop in electrical resistivity known as magnetoresistance (MR). In terms of the equivalent resistance, schematically shown in Figure 1,

$$R^{AP} = \frac{R_\uparrow + R_\downarrow}{2}; \; R^{P} = \frac{2R_\uparrow R_\downarrow}{R_\uparrow + R_\downarrow};$$

$$\mathrm{MR} = \frac{R^{AP} - R^{P}}{R^{P}} \quad \frac{(R_\uparrow - R_\downarrow)^2}{4R_\uparrow R_\downarrow}$$

Thus GMR is defined as $\sigma_P - \sigma_{AP} / \sigma_P$, where σ_P and σ_{AP} are the conductivity of the parallel and anti-parallel configurations respectively.

We shall briefly review the results of our self-consistent supercell electronic structure calculations on Fe/Cr and Ni/Cu are two of the most widely investigated magnetic multilayers because of their technological implication. Also these two systems have also been studied as model systems since they raise interesting fundamental questions, as will be discussed below.

3.1. Ni/Cu multilayer :

Ni/Cu is an interesting model system [26] both from application and fundamental point of view. It was first demonstrated by Bird and Schlesinger [27] that if the thickness of Cu is suitably adjusted in electrodeposited Ni-Cu multilayers, then the ground state is AFM instead of being FM. There was some controversy about the existence of magnetically dead Ni layers at the interface, which was first addressed by Jarlborg and Freeman [28]. In order to understand from first-principles the exact nature of the interlayer magnetic coupling and GMR in the Ni/Cu(100) system, we have carried out spin-polarized (both FM and AFM states) band calculations using TB-LMTO method [29].

The conductivity of the parallel/anti-parallel configurations of the multilayer, can be calculated using semiclassical Boltzmann equation under relaxation time approximation

$$\sigma_{AP(P)} = e^2 \sum \tau_{AP(P)}(k) v_{AP(P)}(k) \delta\left(\epsilon_{AP(P)}(k) - \epsilon_F\right)$$

Here v is the group velocity, τ is the relaxation time, v_F and ϵ_F are Fermi velocity and Fermi energy respectively. Summation is over the wave-vector k. Neglecting k-dependence of τ, the above equation can be simplified as,

$$\sigma_{AP(P)} = e^2 \sum \rho_{AP(P)}(\epsilon_F) v^2_{AP(P)} \tau_{AP(P)} = e^2 D(\epsilon_F) v_F^2 \tau$$

where $D(\epsilon_F)$ is the Fermi level state density. Since the electron mean free path for Cu (~93 Å) is more than the spacer Cu width, the Ni/Cu multilayer is expected to show in-plane GMR due to interface scattering effects.

The Ni_mCu_n (100) multilayer system has been modelled [29] by various $(m + n)$ supercells having body centered tetragonal (bct) structure. Starting from (3+3) supercell, the number of Ni and Cu layers have been progressively increased to form (7+5) and (5+7) supercells. Although Ni and Cu have a lattice mismatch of ~2.5% we have chosen the nearest neighbour Ni-Ni, Cu-Cu and Ni-Cu distances to be same (*viz.* 2.49 Å), thereby neglecting any possible structural relaxation. Since all the structures under consideration are closed packed, the atomic spheres overlaps (≤15%) are well within the permissible limit of ASA. The site – as well as spin-projected DOSs obtained for the different supercells reflect a lot of detailed features of the electronic structure of this system. From the total ground state energies of the supercells calculated for both spin-averaged and spin-polarized configurations, we have estimated the magnetic interaction energy E_{Mag} (meV/atom), defined as $E_{Mag} = (E_{tot}{}^{spin\ pol} - E_{tot}{}^{spin\ av})/(m + n)$ for a $(m + n)$ supercell. For AFM state, the E_{Mag} values turn out to be –14.0, –28.3 and –25.3 meV/atom respectively for (3+3), (7+5) and (5+7) supercell. The corresponding numbers for the FM state are comparable (although these turn out to be consistently higher in magnitude) within the error bar of our present calculations. These results tend to indicate that AFM ordering is one of the possible ground state for Ni/Cu system and also that the magnetic interaction energy for (7+5) supercell is the lowest implying highest relative stability.

Since the AFM state is particularly of interest from the point of view of manifestation of GMR, we have studied the variation of charge transfer and magnetic moment with increase in multilayer thickness. As expected, the central layers for Ni and Cu in (5+7) and (7+5) cases simulate bulk values of charge transfer (Figure 2a) and magnetic moment (Figure 2b) in contrast to the (3+3) case. The Ni layer right at the interface gain a significant amount of charge at the cost of its neighboring Ni as

well as the interfacial Cu layer. As one goes deeper into the Ni layers, the excess charge tend to show Friedel oscillations, while the magnetic moment does not; this is in confirmation with the earlier findings of Jarlborg and Freeman [28]. As required for a RKKY superexchange, the Cu layers do show a slight charge polarization and magnetic moment, for the eventual AFM ordering between the Ni layers. Also the interface Ni layer has a lower magnetic moment (0.37 μB than that of the bulk-like layer (0.6 μB), as expected.

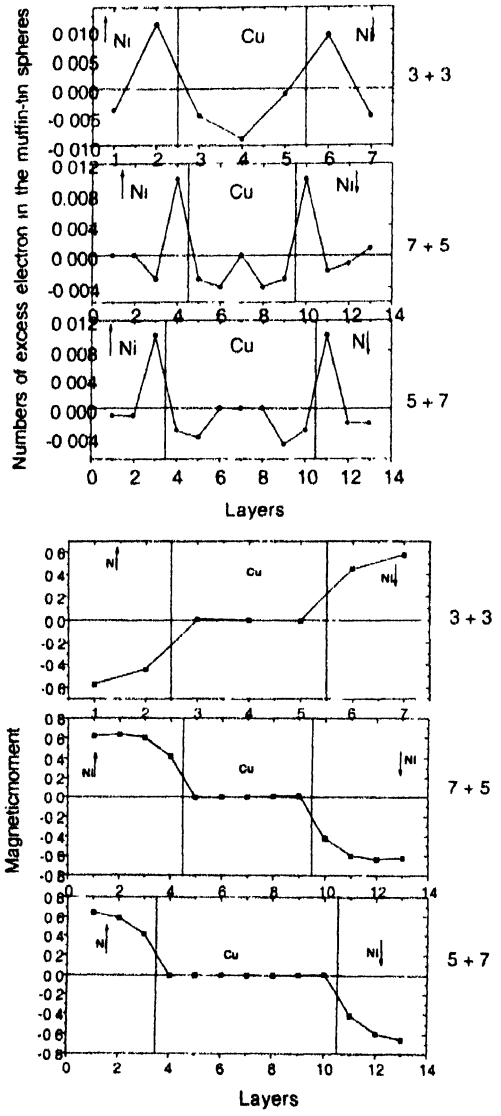

Figure 2. Antiferromagnetically coupled Ni/Cu(100) multilayer : (a) charge transfer and (b) variation of magnetic moment as function of layer thickness.

For the (3+3), (7+5) and (5+7) Ni/Cu multilayers, our calculated in-plane (*i–p*) GMR values are 24.18, 41.21 and 29.90 respectively, while the perpendicular to the plane (*p–p*) GMR values are 37.05, 69.11 and 58.76 respectively [29]. Our results show the same trend as other multilayer GMR systems [26]. The calculated values overestimate the measured values, performed on electrodeposited multilayers [27]. This is partly due to the ideal multilayer model chosen and partly due to the simplifications incorporated in solving the Boltzmann conductivity expression used in our calculation of conductivity.

3.2. *Fe/Cr multilayers :*

Incommensurate spin density wave (SDW) in bulk Cr get affected when several layers of Cr are embedded within ferromagnetic Fe layers in Fe/Cr multilayer system [30]. Experimental studies using perturbed angular correlation and neutron diffraction are not conclusive for thin Fe/Cr multilayers. X-ray circular dichroism results were explained with a model where only Cr atoms close to the Fe interface acquire a significant magnetic moment. Another technique, scanning electron microscopy with polarization analysis has been used for thin Cr layers but is unsuitable for epitaxial Fe/Cr multilayers since Fe/Cr wedges are used in this experiment. It is only recently that a non-magnetic Mössbauer probe *viz.* ^{119}Sn (unlike the conventional ^{57}Fe probe), has been used as a monolayer embedded inside thin Cr layers of Fe/Cr multilayers (*i.e.* Fe/Cr/Sn/Cr multilayers), in order to obtain complementary information about the magnetic hyperfine structures [31]. A large magnetic hyperfine field of 13T was observed at the Sn nuclear sites in Cr(5.0 nm)/Sn(1ML) multilayers, indicating that the magnetic ordering temperature of the Cr layers is much higher than the Neel temperature of bulk Cr (*i.e.* 311 K). It was not clear whether any magnetic moments were induced on the Sn atoms, which in turn convoluted the results for the Cr atoms.

Recently Fe/Cr/Sn/Cr multilayers were grown with a monolayer of ^{119}Sn that serves as nonmagnetic Mössbauer probe inside Cr layers. For thin Cr layers, it was found that the quantum size effect will be prominent and that it will change the magnetic property of Cr [31]. Detailed investigations have been carried out [32–34] to explain the decrease in Cr magnetism with decrease in the Cr layer thickness ranging from ~2 to 30 Å sandwitched between Sn and Fe layers. We have carried out TB-LMTO band structure calculations [32] of the nML (n varying from 15 to 1) Cr layers forming multilayers with 1ML Sn layer, in order to explain the decrease in Cr magnetism with decreasing thickness of the Cr layer. In case of Fe/Cr multilayer, since Fe and Cr are almost lattice matched, one can choose bulk Cr experimental lattice constant 2.88 Å as the in-plane lattice constant, while, the out-of-plane distance for both Cr-Cr and Fe-Cr are chosen as 1.44 Å *i.e.*, half of the bulk Cr lattice constant. For Cr/Sn multilayers, the in-plane equilibrium lattice constants were determined by minimizing the total energy of the supercell, keeping the out-of-plane lattice constant fixed at experimental value 1.57 Å. The later value between Cr and Sn layers, has been arrived at by Mibu *et al* [31] by measurement of structural relaxation. The interplaner separation between Cr layers has been taken as 1.44 Å which is half of the Cr lattice constant. The average Sn layer energy per atom when plotted as a function of the number of Sn layers shows a clear change of the slope at 3 ML-Sn, which corresponds to 6 Å Sn. It can be related with the experimental observation that when Sn layer thickness is set at

6 Å, it looses structural coherency with Cr layers, and β-Sn begins to grow in island growth mode. This inference can be validated by more elaborate total energy calculations.

Figure 3 shows the layer projected DOS (LP-DOS) for Sn/Cr multilayer system with 15 ML Cr layer width and only 1 ML Sn

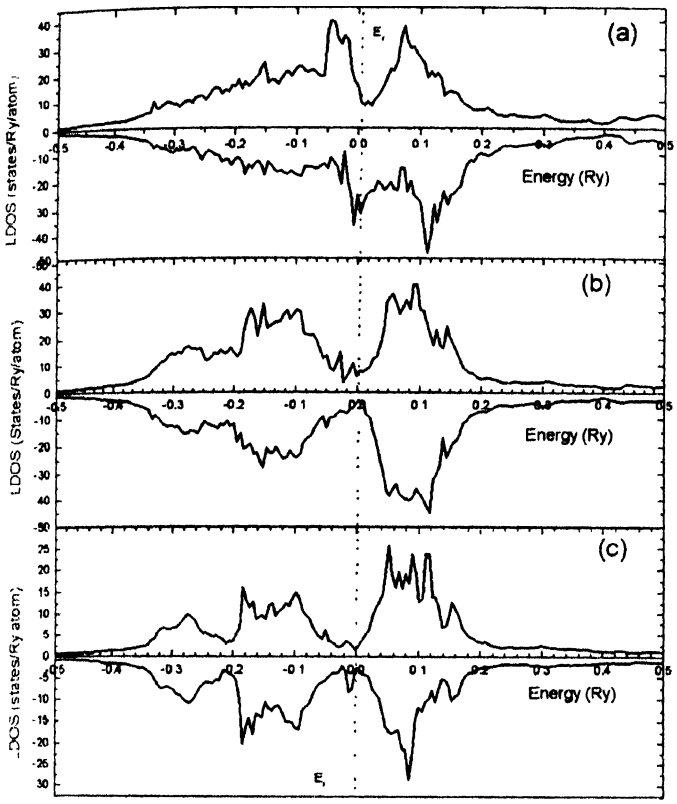

Figure 3. Calculated LP-DOS for Cr (15 ML)/Sn (1 ML) system. (a) The interface Cr layer (b) Next to the interface Cr layer (c) The Cr layer at the centre of the multilayer structure Majority and minority pins are plotted on upper half and lower half of the each graph, respectively.

layer width. From Figures 3(a), (b) and (c) one could see how the basic features of the electronic structure changes while going from central bulk like layer to interfacial layer. Although the main features of the bulk Cr remains unaltered in the central layer (Figure 3(b)); the peaks close to the Fermi energy becomes sharper and new peaks appears whose strength increases while going to the interface layers. Theses are due to the localized interface states. Interface states appear both in majority and minority spin LDOS. The sharp peaky nature of the LDOS below 0.1Ry from the Fermi energy is due to the presence of strain within the multilayer. At the interface (Figure 3(a)) the LDOS structure is completely different from that of the bulk Cr because of reduced symmetry of the interface and the covalent bonding between interface Cr layer and adjacent Sn layer. The LDOS shows large antibonding states slightly below and above the Fermi energy due to the presence of this Sn layer.

Covalent bonding between 5*s* orbital of Sn and 3*d* orbital of Cr is responsible for this antibonding states. For majority spin almost half of the *d*-band which also includes the antibonding states are filled with electrons but for minority spin most of the electrons of the antibonding states are empty. The large magnetic moment is due to the appearance of large number of localized interface states and also due to the presence of Sn atoms as nearest neighbors.

It is seen that the Sn layer acquired some magnetic moment; which is one order of magnitude smaller than that of the adjacent Cr layers and its spin direction is ferromagnetically aligned with Cr layers. Hence the three layers at the interface Cr/Sn/Cr are ferromagnetically aligned which enhances the magnetic moment of interface Cr layer. The increase in density of states at the Fermi surface also indicates the ferromagnetic ordering [35]. In order to ensure the origin of the interface states, we have performed calculation on Fe/Cr multilayer and have compared

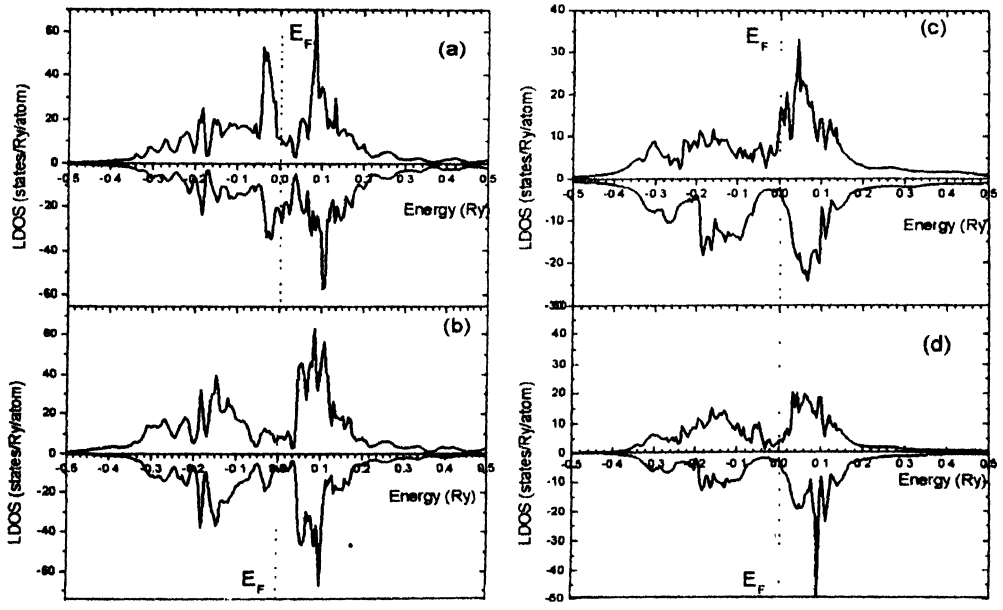

Figure 4. Calculated LP-DOS for Cr (4 ML)/Sn (1 ML) and Fe (3 ML)/Cr (3 ML) multilayer systems. Cr *d* band at the (a) interface layer in Cr/Sn, (b) central layer in Cr/Sn, (c) interface layer in Fe/Cr, and at the (d) central layer in Fe/Cr.

the LDOS of the interface Cr layers in the two cases *viz.* Fe/Cr and Cr/Sn multiplayer systems. Figure 4(a), and (b) show the LDOS for Cr (4ML)/Sn (1ML) and in 4(c) and (d) show the LDOS for Fe (3 ML)/Cr (3 ML). It is cleanly seen that the interface states, which are present in the Cr/Sn multilayer are absent in Fe/Cr multilayer. This is expected, because during growth of Fe/Cr multilayers, Cr atoms diffuse within the Fe layers easily thereby prohibiting the formation of interface state. For this reason it becomes possible to grow monolayer Sn but not of Fe, over multilayers of Cr. In Cr (4 ML)/Sn (1 ML) multilayer, the interface states are stronger than those states appearing for larger Cr thickness (Figure 4). This is expected because in the former case, strain in the interface is much larger than the later multilayers. In both the cases, large number of antibonding states are seen which form a broad hump-like structure near Fermi energy. For smaller layer width of Cr, the reminiscence of the interface and antibonding states are still present in the central layer and hence the magnetism of the Cr layer gets reduced. The states arise due to bonding of 3*d* valence electrons of Fe and Cr are much different from those arising due to bonding between 5*s* and 3*d* electrons of Sn and Cr. The difference between the spin polarization of Sn and Fe gets reflected on the antibonding states of the interface Cr layer. For Fe/Cr, these states alter majority spin electrons much more than minority spin electrons and the result is antiferromagnetic coupling of Fe with Cr.

Figure 5 shows that the local magnetic moments on different Cr layers in Cr (n ML)/Sn (1 ML). The magnetic moments of Cr in for Fe (3 ML)/Cr (3 ML) system are similar to that in Cr (4 ML)/Sn (1 ML) system, so it is not shown separately. It is seen that at first when Cr layer thickness decreases from 15 ML to 8 ML, interface magnetic moment increases by about 12% which is in agreement with the 8% increase in magnetic hyperfine splitting in the Mössbauer experiment. A detailed calculation of the hyperfine field at the Sn site has been done by [34], in order to establish the relationship between increase in magnetic moments and increase in hyperfine splitting. When the Cr layer thickness further decreases, the interaction between Sn-Sn appears (Fe-Fe in case of Fe/Cr multilayer) and due to destructive interference in the reminiscent interface states from both ends of the sandwitched Cr layer the magnetic moments of the thin Cr layers decrease and become zero at 1 ML thickness. All throughout the structures from 15 ML to 4 ML, commensurate antiferromagnetic structure have been observed, which is in agreement with the experimental results.

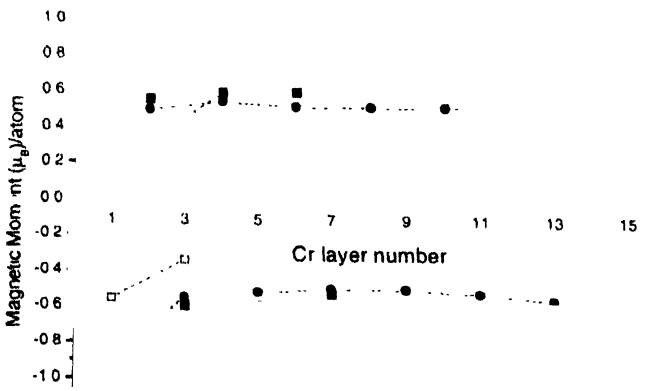

Figure 5. Calculated local magnetic moments of a Cr atom for Cr (*n* ML)/Sn (1 ML) multilayers. Open circle: $n = 15$, open square $n = 8$, open diamond: $n = 4$; magnetic moment of every alternate atoms is connected with dashed lines to show the antiferromagnetic order in the Cr layer. $N = 1,15$ in the Cr (15 ML)/Sn (1 ML) are interface Cr layers, $n = 1,8$ in Cr (8 ML)/Sn (1 ML) are interface Cr layers; and $n = 1,4$ in Cr (4 ML)/Sn (1 ML) are interface Cr layers

4. Concluding remarks

In spite of some of its well-known limitations, local density functional theory is the unchallenged work-horse for electronic structure calculation of materials. It is computationally less demanding compared to Hartree-Fock (HF) based or quantum Monte Carlo (QMC) based calculations, and provide results for bulk solids, surfaces as well as nanostructured materials. With the present day high performance computers, *ab initio* calculations can be performed on systems containing a few 100 atoms at the most, which amounts to length scales of a few nanometers. This is inadequate to probe, for example, novel phenomena that are exhibited in semiconductor structures of carrier lengths of tens of nanometers. For such realistic sizes ($N \sim 10^3 - 10^6$) one has to invoke O(N) procedures where the computational time scales linearly with the system size. There have been several O(N) approaches that have been described in the literature. [36,37] Tight-binding methods [38] are ideally suited in the size range of a few thousand atoms. Beyond this one has to go for some effective medium approach [39]. The density functional molecular dynamics methods, popularly known as Car-Parrinello (CPMD) method [40], is being extensively used for studying the structure and dynamics of various nanostructured materials. Here, the forces on the atoms are derived "on the fly" from the instantaneous ground state of the electrons, obtained *via* self-consistent solution of the many electron Schrödinger equation. Such CPMD techniques extend our capabilities to investigate nano- as well as bio-materials having unknown structure and bonding.

Acknowledgment

I would like to thank my coworkers S K Ghosh, S Mukhopadhyay and H G Salunke for their contributions to the works on metallic multilayers.

References

[1] R W Siegel, E Hu and M C Roco (eds.) *Nanostructure Science and Technology World Technology Evaluation Center (WTEC) Panel Report on R&D Status and Trends in Nanoparticles Nanostructured Materials and Nanodevices* (Kluwer, Dordrecht p335 (1999)

[2] P G Collins, M S Arnold and P Avouris *Science* **292** 706 (2001)

[3] K Eric Drexler *Engines of Creation : The Coming Era of Nanotechnology* (Anchor Books, 1987); K Eric Drexler, Chris Peterson and Gayle Pergamit, *Unbounding the Future the*

Nanotechnology Revolution (New York : William Morrow and Company, Inc.) (1991)

[4] L Esaki and R Tsu *IBM J. Res Develop* **14** 61 (1980), *Int J. Mod Phys.* **B3** 487 (1989)

P E Blöchl, C Joachim and A J Fisher (eds.) *Computations for the Nano-scale, Nato Science Series E 240* (Dordrecht : Kluwer Academic Publishers) (1993)

A Mookerjee and D D Sarma (eds) in *Electronic Structure of Alloys, Surfaces and Clusters* (London : Taylor & Francis) (2003) see articles therein

W G Richards and D K Cooper *Ab initio Molecular Orbital Calculations for Chemists* (Oxford : Clarendon Press) (1985)

[8] K Kitaura *et al, Chem Phys Lett* **336** 163 (2001)

[9] R Santamaria *et al, Phys. Rev* **A64** 042501 (2001)

[10] L Colombo *et al* (eds), *Advances in Materials Theory and Modeling : Bridging Over Multiple-Length and Time Scales Mat Res Soc. Symp Proc* **Vol. 677** (2001)

[11] G H Johanesson, T Bligaard, A V Ruban, H K Skriver, K W Jacobsen and J K Norskov *Phys Rev Lett.* **25** 255506 (2002)

[12] W Kohn and L J Sham *Phys Rev* **140** A1133 (1965)

[13] S Lundqvist and N H March (eds) *Theory of Inhomogeneous Electron Gas*, (New York : Plenum) (1983)

[14] R O Jones and O Gunnarsson *Rev. Mod. Phys* **61** 689 (1989)

[15] O K Andersen and O Jepsen *Phys. Rev Lett* **53** 2571 (1984)

[16] G P Das *Pramana-J Phys* **38** 545 (1992), G P Das in *Methods of Electronic Structure Calculations* (eds) V Kumar, O K Andersen and A Mookerjee (World Scientific) p279 (1994)

[17] G P Das in *Electronic Structure of Alloys, Surfaces and Clusters* (eds) A Mookerjee and D D Sarma (London : Taylor & Francis) (2003) pp22-70 and references therein

[18] G P Das in *Materials Research : Current Scenario and Future Projections* (eds.) R Chidambaram and S Banerjee (New Delhi Allied Publisher) p634 (2003)

G P Das, P Blochl, O K Andersen, N E Christensen and O Gunnarsson *Phys Rev Lett* **63** 1168 (1989)

[20] H van Leuken, A Loder, M T Czyzyk, F Springelkamp and R A deGroot *Phys Rev.* **B41** 5613 (1990)

[21] B Y Jin and J B Ketterson *Adv Phys* **38** 189 (1989)

[22] M N Baibich, J M Broto, A Fert, V D Nguyen, P Etienne, G Creuzet, A Friederich and J Chazelas *Phys Rev Lett* **61** 2472 (1988)

[23] M van Schilfgaarde and F Herman *Phys Rev Lett* **71** 1923 (1993)

[24] P Bruno *Phys Rev* **B52** 411 (1995)

[25] M A M Gijs and G E W Bauer *Adv Phys* **46** 285 (1997)

[26] T Kai, Y Ohashi and K Shiiki *J Mag Mag Mater* **183** 292 (1998)

[27] K D Bird and M Schlesinger *J Electrochem Soc* **142** L65 (1995)

[28] T Jarlborg and A J Freeman *Phys Rev Lett* 45 653 (1980)

[29] S K Ghosh, H G Salunke, G P Das, A K Grover and M K Totlani *Bull Mater Sci* **22** 761 (1999)

[30] R S Fishman *J Phys Cond Matter* **13** R235 (2001)

[31] K Mibu, S Tanaka and T Shinjo *J Phys Soc J* **67** 2633 (1998), K Mibu, M Almokhtar, S Tanaka, A Nakanishi, T Kohayashi and T Shinjo *Phys Rev Lett* **84** 2243 (2000)

[32] S Mukhopadhyay, G P Das, S K Ghosh, A Paul and A Gupta *J Magn Magnetic Mater.* **246** 329 (2002)

[33] S Mukhopadhyay and D Nguyen-Manh *Phys Rev* **B66** 144408 (2002)

[34] H Momida and T Oguchi *J Mag Magn Mater* **234** 126 (2001)

[35] H L Skriver *J Phys* **F11** 97 (1981)

[36] S Goedecker *Rev Mod Phys* **71** 1085 (1999)

[37] S Y Wu and C S Jayanthi *Phys Rep* **358** 1 (2002)

[38] C M Goringe, D R Bowler and E Hernandez *Rep Prog Phys* **60** 1447 (1997)

[39] R M Nieminen, M J Puska and M J Manninen (eds) *Many-Atom Interactions in Solids* (Berlin : Springer Verlag) (1990)

[40] R Car and M Parrinello *Phys Rev Lett* **55** 2471 (1985)